

1 Supplementary Material

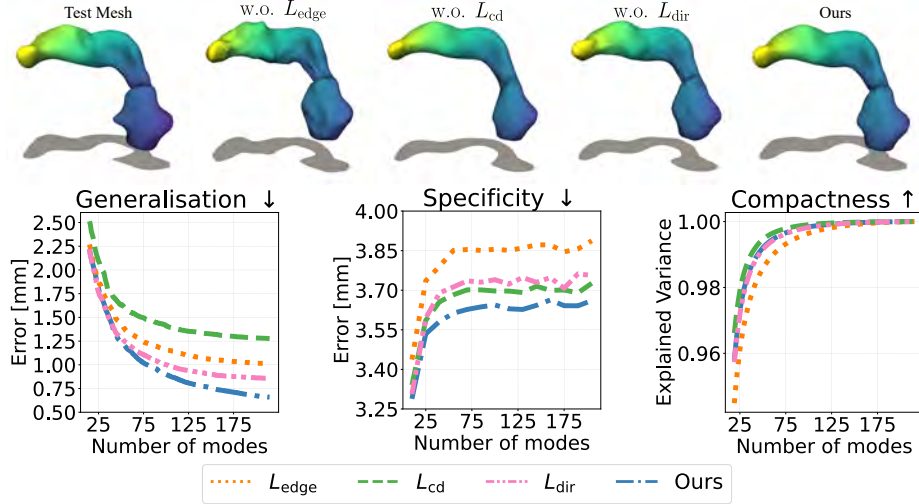


Fig. S1. Ablation study on the pancreas dataset. (Top) Reconstruction of a test mesh using our method trained without individuals terms of our deformation coherency loss introduced Eq. (4) (i.e. L_{edge} , L_{cd} , L_{dir}). The reconstruction using our full method (all three losses) achieves the best qualitative results. (Bottom) Generalisation, specificity of compactness of our method trained with and without L_{edge} , L_{cd} , L_{dir} .

Table S1. Implementation details for our method. The last four rows (denoted by *) are details from the SmS framework. See [7] for more details.

Implementation details	Value	Loss	Weight
Epochs	15	L_{cd}	10^{+4}
Time steps K	6	L_{dir}	10^{+2}
GPU	NVIDIA A100	L_{edge}	10^{+5}
Optimizer for DiffusionNet*	Adam with lr 10^{-3}	L_{struct} *	1
Optimizer for ResnetECPos*	Adam with lr 10^{-3}	L_{couple} *	1
Number of eigenfunctions*	40	L_{symm} *	1
τ for PMap computation*	0.07	L_{align} *	10

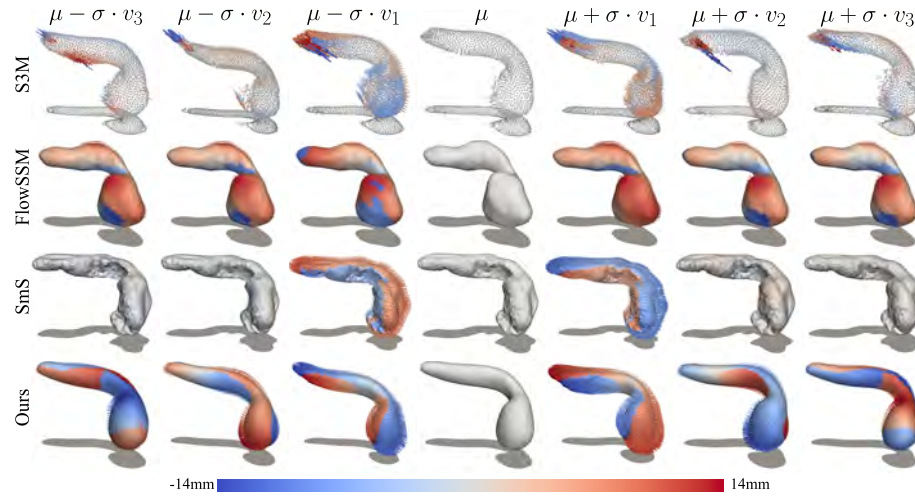


Fig. S2. Top three PCA modes of variations identified by S3M [3], FlowSSM [16], SmS [7] and our proposed method. Our method can operate on the head, neck, and body of the pancreas using just the first three modes of variation. The colour map and arrows show the signed distance and direction from the mean shape.



Fig. S3. Random samples created using our method. The shape diversity of the samples showcases our method’s ability to capture the biological variability of the training data (low specificity errors).

Table S2. Additional information on the datasets [25, 26] used in our paper.

Organ	Scans	Curated from
Pancreas	273 segmented CT	patients undergoing resection of pancreatic masses
Spleen	41 segmented CT	patients with metastatic liver disease
Liver	131 segmented CT	patients receiving chemotherapy for liver metastases
Hippocampus	260 segmented MRI	a combination of healthy adults and individuals with non-affective psychiatric disorders
Lung	subset of 126 segmented CT	patients with pulmonary nodules